X-ray flare sparks quake inside Sun

Solar flares involve a release of the Sun's magnetic energy as X-radiation, particle beams and high-speed plasma flows. But we have discovered, using data from the Solar and Heliospheric Observatory (SOHO), that these flares also affect the Sun's interior, generating seismic waves similar to earthquakes. For example, a three-kilometre-high seismic wave was caused by a moderate X-ray flare that occurred on 9 July 1996 and propagated at about 50 kilometres per second to a distance 120,000 kilometres from the flare site.

This seismic response was stronger than would be expected, both from the current model of flares as giant electromagnetic explosions in the upper chromosphere and corona, and from previous attempts to detect the seismic response in ground-based data[1,2]. The solar surface is covered by low-frequency (3 millihertz) sound waves that are stochastically excited in millions of small convective elements. These waves have been used to probe the large-scale structures of the Sun's interior[3]. Despite having different causes, the disturbances resulting from solar flares are fairly similar to earthquakes in many respects, for example in the impulsive localized release of energy and momentum.

The flare of 9 July was the only significant X-ray flare observed in 1996 and was of moderate size. At times of maximum solar activity, flares several times larger can be observed, which would shake the Sun more strongly.

The X-ray impulse of this flare (classified as X2.6/lB) was first detected by the Burst and Transient Source Experiment (BATSE) on board the Compton Gamma Ray Observatory at 09:07:49 UT and reached a sharp maximum at 09:09:40 (Fig. 1a). The magnetic field measurements from the Michelson Doppler Imager (MDI)[4] instrument on SOHO show that the flare was associated with emerging flux of opposite polarity in the active region NOAA 7978 a few hours before the flare.

MDI dopplergrams reveal strong localized upward and downward mass flows during the X-ray impulse (Fig. 1b), 3–5 megametres (Mm) across. The velocity impulse was almost as sharp as the X-ray flux, but the maximum velocity was not observed until about 1 min after the X-ray maximum, at 09:11:00. This delay is consistent with theoretical predictions based on the 'thick-target' model of solar flares[5–8], which predicts a strong downward propagating shock following a high-energy electron beam heating the cool chromospheric 'target'. The impact of this shock causes the seismic response.

We have also detected flare ripples, circular wave packets propagating from the flare and resembling ripples from a pebble thrown into a pond. The seismic wave was first detected at about 09:30, 20 minutes or so after the flare, at about 18 Mm from the flare. The wave was observed in a sequence of dopplergrams for about 35 minutes, after which the amplitude dropped rapidly (Fig. 1c).

We have constructed seismograms of the solar flare by remapping the Doppler images into polar coordinates centred at the point of the initial velocity impulse, and then applying a Fourier transform with respect to the azimuthal angle (Fig. 1d). A circular disturbance produced a set of ridges with a positive slope. The ridges began about 18 Mm from the flare at 09:32 and reached about 120 Mm at 10:02. The velocity of the wave packet increased from about 30 km s^{-1} to about 100 km s^{-1} as the wave moved from 20 to 120 Mm from the epicentre.

We have compared these observations with theoretical models of the flare seismic response, which predict similar ripples[9]. The maximum theoretical amplitude matches the observation if the shock momentum transported to the photosphere in a downward propagating shock wave is about 3×10^{22} g cm s^{-1}. This is larger than the flare momentum typically estimated from spectral observations[7,10].

The dipole component of the flare wave does not have a significant signal, but the quadrupole component shows ridges at distances from 15 to 40 Mm from the flare, which presumably result from scattering on the magnetic structures of the active region.

The detection of seismic responses to solar flares opens interesting prospects for flare seismology and for determining the effects of flare processes in the Sun's interior. Substantially stronger and larger X-ray flares are observed in other stars; detection of 'star-quakes' caused by such flares might be an interesting challenge for stellar astronomy.

A. G. Kosovichev
W. W. Hansen Experimental Physics Laboratory, Stanford University, Stanford, California 94305-4085, USA
V. V. Zharkova
Department of Physics and Astronomy, Glasgow University, Glasgow G12 8QQ, UK

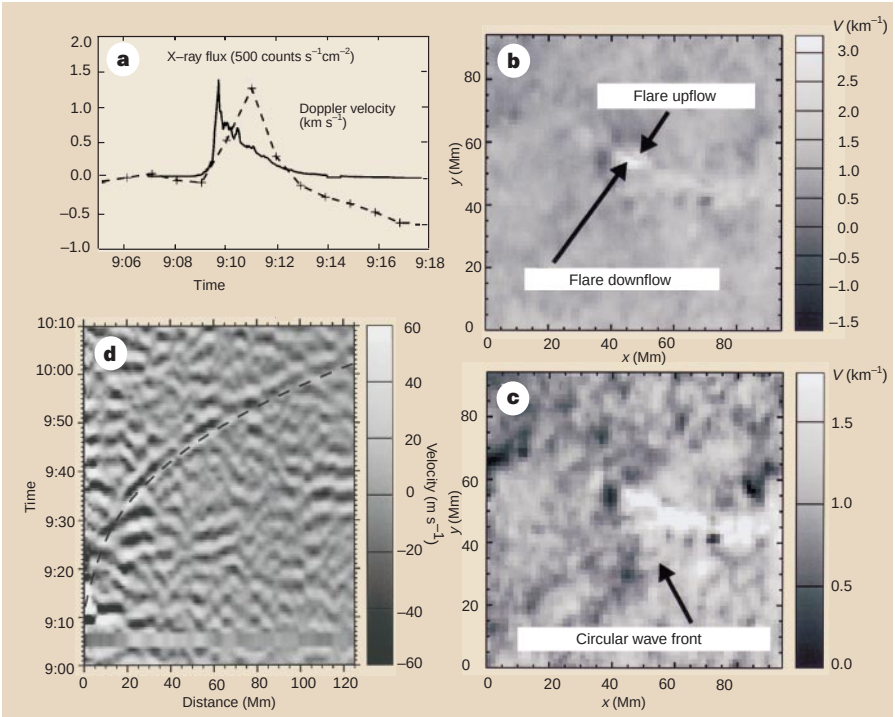

Figure 1 Characteristics of the solar flare of 9 July 1996. **a,** The X-ray flux in the energy range 25–100 keV from the BATSE flare monitor (solid curve), and the 1-minute averages of the Doppler velocity of the downflowing plasma in the flare core from the MDI (dashed curve with crosses). **b, c,** The MDI dopplergrams of the flare region showing the line-of-sight velocity (**b**) immediately after the X-ray pulse at 09:11 and (**c**) when the flare wave reached maximum amplitude at 09:37. Bright areas, downflows; dark areas, upflows. **d,** Flare seismogram representing the axisymmetrical components of the velocity disturbance. Dashed curve, theoretical time–distance relation for acoustic rays initiated at the flare core at 09:11; the flare signal is a black-and-white ridge around this curve. Other disturbances are solar noise.

1. Haber, D. A., Toomre, J., Hill, F. & Gough, D. O. in *Proc. Symp. Seismology of the Sun and Sun-like Stars,* Tenerife, Spain, 26–30 September, ESA SP-286, 301–304 (1988).
2. Braun, D. C. & Duvall, T. L. Jr *Sol. Phys.* **129,** 83–94 (1990).
3. Kosovichev, A. G. *et al. Sol. Phys.* **170,** 43–61 (1997).
4. Scherrer, P. H. *et al. Sol. Phys.* **162,** 129–188 (1995).

5. Kostyuk, N. D. & Pikel'ner, S. B. *Sov. Astronomy* **18,** 1002–1016 (1975).
6. Kosovichev, A. G. *Bull. Crimean Astrophys. Observatory* **75,** 6–18 (1986).
7. Zarro, D. M., Canfield, R. C., Strong, K. T. & Metcalf, T. R. *Astrophys. J.* **324,** 582–589 (1988).
8. Zharkova, V. V. & Brown, J. C. in *Solar Dynamic Phenomena and Solar Wind Consequences,* Proc. 3rd SOHO Workshop, ESA SP-373, Noordwijk, 61–65 (1994).
9. Kosovichev, A. G. & Zharkova, V. V. in *Helioseismology,* Proc. 4th SOHO Workshop (eds Hoeksema, J. T., Domingo, V., Fleck, B. & Battrick, B.), ESA SP-376, Noordwijk, 341–344 (1995).
10. Canfield, R. C., Zarro, D. M., Metcalf, T. R. & Lemen, J. R. *Astrophys. J.* **348,** 333–340 (1990).

Low nitrate:phosphate ocean ratios corrected...

It has become apparent, since publication of our Letter on low nitrate:phosphate ratios in the global ocean (T. Tyrrell and C. S. Law, *Nature* **387,** 793–796; 1997; correction, **393,** 396; 1998), that the World Ocean Atlas 1994 (WOA94) database we used contains transcription errors for nutrient measurements. Discrepancies between the original data and the corresponding data sets in WOA94 have been confirmed for the eastern tropical Pacific (identified by A. Longhurst and S. Sutherland), the western North Pacific (M. Aoyama, K. Hirose and K. Ishikawa) and the Agulhas retroflection area south of South Africa (R. Schlitzer and A. Longhurst).

Removal of falsely identified low nitrate:phosphate points (LNP, $([NO_3^-] \div [PO_4^{3-}]) < 3.0$ and $[PO_4^{3-}] > 1.5$ μmol kg^{-1}) in these areas shows that: (1) LNP points do not occur in the open ocean away from the coast; and (2) the western and northern North Pacific does not represent a hitherto-unquantified significant site for denitrification, as we originally suggested.

However, by examining other independent and more rigidly controlled data sets and re-evaluating WOA94 data using stricter criteria, we have confirmed that LNP is a feature of the Baltic and Black Seas, the Peruvian upwelling system, the Cariaco trench, the Bering Straits, and Tomales Bay. Although this confirms our original premise that the Redfield ratio is not universally applicable, it is clear that LNP points are restricted to coastal and enclosed shelf sea regions. These observations accord with current understanding of the extent of denitrification.

We thank those named above for detecting data discrepancies, and Steve Smith, Louis Codispoti, Geoff Bailey, Sergey Konovalov, Lee Cooper, Peter McRoy, Chirk Chu, Jean Garside, Chris Garside, Gwo-Ching Gong, Alexander Bychkov and Mikael Krysell for sending data sets.

T. Tyrrell
Department of Oceanography, Southampton Oceanography Centre, University of Southampton, European Way, Southampton SO14 3ZH, UK

C. S. Law
Plymouth Marine Laboratory, Prospect Place, Plymouth PL1 3DH, UK

...and database flagged

The errors in the World Ocean Atlas 1994 that were identified as a result of the publication of Tyrrell and Law's Letter (T. Tyrrell and C. S. Law, *Nature* **387,** 793–796; 1997) are, as part of our routine quality-control procedures, being corrected or flagged as suspect on this and related National Oceanographic Data Center databases.

Margarita Conkright
Ocean Climate Laboratory, OC5, National Oceanographic Data Center, 1315 East West Highway, Silver Spring, Maryland 20910-3282, USA

Global impact of the 1789–93 El Niño

It has been suggested that global warming has caused the El Niño/Southern Oscillation (ENSO) climatic events to become more frequent and intense. However, several ENSO events that occurred before 1880 had effects at least as intense and wide-ranging as those associated with the current event. This is the case particularly for the events in 1396 (ref. 1), 1685–88, 1789–93 and 1877–79. Here I discuss archival evidence, notably from South Asia and above all for the 1789–93 ENSO, for the strength of these historical effects.

In peninsular India, every major drought between 1526 and 1900 has been closely associated with the eastern Pacific El Niño. The 1789–93 ENSO event produced prolonged droughts, especially in South Asia, a region where the association between ENSO and the monsoon is well established[2]. The global impact of this event was recognized in 1816 by Alexander Beatson, governor of St Helena, who suggested that the 1791 droughts in India, St Helena and Montserrat were part of a single, connected phenomenon[3].

The earliest indications of the event in the tropics were meteorological observations, based on a 14-year data set started in the early 1770s by William Roxburgh at Samulcottah (Samalkot) in southern India[4]. He recognized the exceptional nature of the droughts beginning in 1789 and believed that their severity had only been approached by those in 1685–87 (ref. 5). Those years are now known to have been characterized by 'very severe' El Niño in the eastern Pacific in 1687–88 (ref. 6).

Roxburgh recorded the continuous failure of the South Asian monsoon between 1789 and 1792, the severest failure being in 1790 (Table 1). The first major rainfall reduction was in 1789 in southern India, more than a year before similar droughts occurred in Australia, Mexico, the Atlantic islands and southern Africa. By November 1792, 600,000 deaths were attributed to the resultant droughts in the northern Madras Presidency alone, where half the population died.

The long droughts were interspersed with short periods of highly destructive rainfall. In three days at Madras in late October 1791, 25.5 inches of rain fell, "more than… has been known within the memory of man"[7]. Unseasonal severe droughts were experienced in Java, and in New South Wales, Australia, in the same year. On 5 November 1791, the governor of this colony, Arthur Phillip, reported that the normally perennial 'Tank Stream' river flowing into Sydney Harbour had been dry for "some months". It did not flow again until 1794. Phillip marks the start of the droughts in July 1790; no rain had fallen by August 1791 (ref. 8).

In Mexico, the level of Lake Pátzcuaro fell steadily between 1791 and 1793, giving rise to disputes over the ownership of the land that emerged[9]. By mid-August 1791, the desiccating effects on the islands of the Antilles were the severest since 1700, and no rain had fallen on the islands of St Vincent and Montserrat[10]. The drought continued on Montserrat until November 1792.

Droughts on St Helena were later than those in the Caribbean, lasting from late 1791 to mid-1794. The River Nile fell to very low levels from 1790 to 1797, as a result of reduced rainfall in the Ethiopian highlands. Evidence from the rest of Africa is scanty, but prolonged droughts in Natal and Zululand between 1789 and 1799 resulted in the *Mahlatule* famine, the severest known to have affected Southern Africa before 1862 (ref. 11).

This evidence that the 1789–93 ENSO had a strong global impact indicates that it was

Table 1 **Monthly rainfall at Samulcottah, Andhra Pradesh, India: May–November 1788–92 (in inches and twelfths of an inch)[15]**

	1788	1789	1790	1791	1792
May	15.4	1	–	4	3.6
June	7.2	6	1.8	4.1	5
July	22.3	6.10	4.9	5.6	6.4
August	12.2	21.1	3.8	–	1.8
September	8.9	1.4	4.8	3.9	7.5
October	5.9	10.1	1.5	3.3	13.11
November	6	1.3	1.2	6.4	–
Total	77.5	43.10	17.4	26.11	37.10